NASA Technical Memorandum 105897

Performance and Heat Transfer Characteristics of a Carbon Monoxide/Oxygen Rocket Engine

Diane L. Linne
Lewis Research Center
Cleveland, Ohio

February 1993

NASA

Performance and Heat Transfer Characteristics of a Carbon Monoxide/Oxygen Rocket Engine

Diane L. Linne
National Aeronautics and Space Administration
Lewis Research Center
Cleveland, Ohio 44135

ABSTRACT

The combustion and heat transfer characteristics of a carbon monoxide and oxygen rocket engine were evaluated. The test hardware consisted of a calorimeter combustion chamber with a heat sink nozzle and an eighteen element concentric tube injector. Experimental results are given at chamber pressures of 1070 and 2070 kPa, and over a mixture ratio range of 0.3 to 1.0. Experimental C* efficiency was between 95 and 96.5 percent. Heat transfer results are discussed both as a function of mixture ratio and axial distance in the chamber. They are also compared to a Nusselt number correlation for fully developed turbulent flow.

INTRODUCTION

The future exploration of the solar system will require the launch of large masses from the surface of the Earth. If chemical propulsion is used for these travels, then a significant percentage of this launch mass will consist of propellants for the outbound trip and the journey home. One proposal to reduce launch mass requirements is to eliminate the need to launch the return propellants (and some of the outbound propellant used to carry the return propellants) by producing these propellants at the site of exploration. This utilization of indigenous materials for propulsion has recently garnered much attention among mission planners, who show that in situ propellants can reduce the Earth launch mass for a lunar or Mars mission by 30 to 66 percent (refs. 1-7). The propulsion technology base for some of the proposed propellants, however, needs to be enlarged before an actual engine can be developed.

The atmosphere of Mars consists of over 95 percent carbon dioxide. One proposed method for utilizing this resource is by dissociating the CO_2 into oxygen and carbon monoxide, and then recombining these propellants in a rocket engine. Although carbon monoxide has been burned in several applications, such as the catalytic converter in an automobile engine, specific experimentation to obtain the information necessary to design a flight engine has only been performed to a limited extent (refs. 8,9). The ignition characteristics of a dry carbon monoxide/oxygen mixture in a spark torch igniter were studied, and an ignition range identified (ref. 8). Additionally, steady-state combustion has been demonstrated in heat sink hardware, and some preliminary combustion efficiencies obtained (ref. 9).

Because of the limited database, tests were conducted with a calorimeter combustion chamber to study the heat transfer characteristics of the oxygen and carbon monoxide propellant combination. The objectives of the experiment were to measure the combustion efficiency with a newly designed 18 element concentric tube injector, and to obtain hot-gas-side heat flux data. The combustion efficiency is compared with results from a previous experiment (ref. 9), and with theoretical predictions of real-engine losses. The heat transfer results are shown together with a Nusselt number correlation for fully developed turbulent flow.

TEST APPARATUS AND PROCEDURE

Test Facility

The experimental tests for this study were performed in Cell 21 of the Rocket Lab at the NASA Lewis Research Center. This

facility contains a low thrust rocket engine test stand with supporting fluid systems that allow precise flow control. Four separate gaseous propellant lines were used for this research program: one oxygen supply line to the engine, one oxygen supply line to the spark torch igniter, one carbon monoxide fuel supply line to the engine, and one hydrogen fuel supply line to the igniter.

The flow rate of each of the gases in the system described above was controlled with a sonic orifice. Inserted as a component of the propellant line, each orifice insured a constant flow rate of gas, independent of downstream pressure perturbations. By measuring the line pressure and temperature at a point just upstream of each sonic orifice, gas flow rates were calculated. Different diameter orifices could be easily interchanged in the system so that the gas flow rate range could be varied throughout the test program.

Test Hardware

The test hardware for this experiment consisted of an igniter, injector, calorimeter chamber spool piece, and converging-diverging nozzle. Figure 1 shows a schematic of the test apparatus and figure 2 shows the hardware on the test stand.

A hydrogen-oxygen spark torch igniter was used to initiate combustion. Gaseous oxygen and gaseous hydrogen were injected into the igniter chamber at an oxygen-to-fuel mixture ratio (O/F) of approximately 40, where a standard spark plug initiated combustion. The hot gases then travelled down a tube through the center of the injector body and into the combustion chamber. At the exit of the igniter tube, additional gaseous hydrogen, which had been used to cool the outside of the igniter tube, was added to the hot gases to increase the flame temperature. This additional hydrogen lowered the total igniter mixture ratio at the exit of the igniter tube to approximately 6.0.

An 18 element concentric tube injector was used for the combustion chamber. Each element injected oxygen through the center orifice and carbon monoxide through the outer annulus. The elements were arranged in two circles centered around the igniter, with six elements on the inner circle and twelve elements on the outer circle (figure 1b). Chamber pressure was measured by means of a pressure tap on the face of the injector.

The calorimeter test chamber was 14.9 cm (5.875 inches) long and had a 6.6 cm (2.6 inches) inside diameter. The inner copper liner was cooled by 46 circumferential cooling channels. Coolant water was supplied to these channels by 22 inlet tubes. Heat flux was calculated at each of the 22 stations by measuring the coolant inlet and outlet temperatures, the coolant flow rate, and the chamber wall area cooled by those channels. In order to obtain an axial temperature profile, two thermocouples were inserted into the copper liner to within 0.0762 cm (0.030 inches) of the hot-gas-side wall at 11 axial locations. Table 1 lists the axial location of the coolant circuits and the thermocouples.

A copper heat sink converging-diverging nozzle was used. The nozzle had a throat diameter of 1.143 cm (0.45 inches) and an exit area ratio of 2.997. The diverging nozzle contour was a cone, with an exit half-angle of 15 degrees.

Test Procedure

To insure a uniform run profile throughout the duration of the test program, each firing of the engine was sequenced by a programmable line controller. Each test run started with the initiation of the oxygen and hydrogen flows to the igniter, followed by the oxygen and carbon monoxide flows to the main combustion chamber after the igniter spark was started. After initiation of main combustion, the igniter was stopped, and the test continued for approximately 6 seconds with no hydrogen flowing. This sequencing allowed for hydrogen to be present during start-up of the engine to aid in the ignition of the dry carbon monoxide and oxygen mixture.

The oxygen flow rate was varied from 21 to 94 g/sec (.046 to .21 lbm/sec). The carbon monoxide flow rate was varied from 47 to 144 g/sec (.104 to .317 lbm/sec). The total flow rate was held relatively constant at 95 and 186 g/sec (.21 and .41 lbm/sec) which provided actual chamber pressures of approximately 1070 and 2070 kPa (155 and 300 psia).

Experimental data was gathered during the test runs by a high-speed data acquisition system. In addition to the instrumentation on the hardware, pressure transducers and thermocouples were applied to the facility feed systems to properly measure the propellant flow rates and temperatures. A total of 100 instrumentation channels were each scanned at the rate of 100 times per second. Each value quoted in this analysis is an average of 10 readings of the instrument by the data system. The data reduction was performed by a FORTRAN 77 computer program hosted on a VAX cluster.

DESCRIPTION OF COMPUTER CODES

Two computer codes were used during evaluation of the experimental results. The Liquid Propellant Program (LPP) computer code (ref. 10) was used for characteristic velocity (C*) efficiency and heat flux comparisons. The Rocket Engine Heat Transfer Evaluation Program (REHTEP) (an unpublished, NASA Lewis Research Center computer code) was also used for heat transfer characteristics comparisons.

Liquid Propellant Program

The LPP code uses a chamber and nozzle geometry together with thermodynamics and kinetics to calculate various performance losses that an actual engine may experience in normal operation. The code consists of several modules, each of which models a different type of performance loss. All modules assume complete combustion in the chamber, that is, no loss in energy release caused by slow vaporization or nonuniform mixing.

The Mass Addition Boundary Layer (MABL) module was used to calculate C* efficiencies and chamber heat flux. This is a boundary layer module that models the growth of the viscous boundary layer in the chamber and nozzle. For this analysis, the start of the boundary layer was assumed to be at the injector. The MABL module uses output from the previous modules, especially the Two Dimensional Kinetics (TDK) module, which predicts the inviscid, two-dimensional expansion of the gaseous combustion products assuming finite-rate kinetics. To simulate the expected wall conditions, the actual wall temperature profile measured in the experimental tests was used as input. For the theoretical analyses presented in this paper, MABL calculates the displacement thickness for the actual chamber and nozzle geometry and uses this to obtain a displaced, or inviscid, wall contour. The TDK module is then rerun with the new contour. A new mass flow rate is obtained and this mass flow is then used along with the actual or geometric throat area to obtain a predicted value of C*. This value of C* is divided by the theoretical ideal value of C* to obtain a theoretical C* efficiency. MABL also calculates the heat flux at the chamber wall, and these values were used for comparison to the experimental results.

Rocket Engine Heat Transfer Evaluation Program

The REHTEP code uses a chamber and nozzle geometry together with specifications for axial coolant passages to evaluate heat transfer characteristics and cooling capabilities of various propellant combinations and coolants. The program calculates the conditions (combustion products, temperature, and other thermodynamic properties) in the engine using a one dimensional equilibrium subroutine. With these values, a heat transfer coefficient is calculated using a Nusselt number correlation for fully developed turbulent flow

$$Nu = \frac{h_g * D}{k_g} = C_g * \mathrm{Re}^{.8} * \mathrm{Pr}^{.3} \qquad (1)$$

where h_g is the heat transfer convection coefficient, D is the diameter of the chamber, k_g is the conductivity of the combustion gases, C_g is the correlation coefficient (0.026 was used in this study), Re is the Reynolds number, and Pr is the Prandtl number. In this program, the transport properties are evaluated at Eckert's reference enthalpy (ref. 11). The heat flux at the chamber wall is then calculated using an assumed wall temperature and the heat transfer equation

$$Q = h_g * \left(T_{aw} - T_{gw}\right) \tag{2}$$

where Q is the heat flux per unit area, T_{aw} is the adiabatic wall temperature, and T_{gw} is the temperature of the chamber wall. The theoretical adiabatic wall temperature is corrected for combustion efficiency, which is an input to the program. The wall temperature is then iterated upon until an energy-balance between the coolant side and the combustion side of the chamber is achieved.

RESULTS AND DISCUSSION

Two types of experimental data, performance and heat transfer, were of interest to meet the objectives of the test program. Experimental C* efficiency results from this test series are compared to previously obtained experimental data, and to efficiencies obtained from the LPP program. The heat transfer results included chamber wall temperatures and chamber heat flux. Experimental results are discussed as functions of mixture ratio and axial distance in the combustion chamber and are also compared to results obtained from the two computer codes.

C* Efficiency

In a previous experimental test program (ref. 9), C* efficiencies of 89 to 92 percent were obtained. In those tests an eight-element triplet injector design was used. For this test program, an eighteen-element, concentric tube injector was designed in an effort to increase the combustion C* efficiency. The injector face is shown schematically in figure 1b.

Figure 3 shows the experimental C* efficiencies as a function of mixture ratio obtained from both injectors, along with a C* efficiency obtained from the boundary layer module of the Liquid Propellant Program (LPP). The computer program calculated real engine losses for the test hardware, and predicted C* efficiencies between 96 and 97 percent over the mixture ratio range of 0.3 to 1.3 (stoichiometric mixture ratio = 0.571). The experimental efficiencies obtained with the concentric tube injector were between 95 and 96.5 percent. The figure shows that the experimental efficiencies were higher at the lower mixture ratios where the fuel to oxygen injection velocity ratio was higher, providing for better mixing between the carbon monoxide and oxygen. The figure also shows that the efficiencies obtained with the concentric tube injector are a significant improvement over those obtained in the previous test program.

Heat Transfer Characteristics

The heat transfer characteristics of the test hardware were evaluated in two manners. First, experimental chamber heat flux was examined as a function of mixture ratio and as a function of axial distance from the injector. Second, the experimental heat flux results were compared to heat flux calculated from boundary layer theory and from a Nusselt number correlation for fully developed turbulent flow in a constant area duct.

Experimental Results. The experimental heat flux, q, in the chamber was calculated based on the temperature rise of the coolant water and the coolant water mass flow rate

$$q = \frac{m_c * C_p * \left(T_{co} - T_{ci}\right)}{A} \tag{3}$$

where m_c is the coolant water mass flow rate through that circuit, C_p is the specific heat of water, T_{co} is the coolant outlet temperature, T_{ci} is the coolant inlet temperature, and A is the chamber wall area cooled by that circuit. This

method of calculation assumes only radial conduction in the copper liner. To reduce the amount of axial conduction, the coolant water flow rates for each coolant circuit were adjusted until the chamber wall temperatures were approximately equal between adjoining stations. Figure 4 shows the wall temperatures, as measured by the rib thermocouples, for a typical test run for each chamber pressure. The figure shows that for the tests run at a chamber pressure of 1070 kPa, the wall temperatures were within five degrees of 355 K, with the exception of the first and last thermocouples (station 2 and station 21). Because the heat flux at these stations was significantly lower than the rest of the stations, it was difficult to adjust the coolant water flow rate low enough to obtain the same wall temperature. Similar results were obtained for the tests run at a chamber pressure of 2070 kPa, where the wall temperatures were within five degrees of 360 K.

The experimental heat flux as a function of mixture ratio is shown in figure 5 at an axial location of 5.268 cm (2.074 inches, cooling station 8) and of 14.16 cm (5.574 inches, cooling station 22). Cooling station 8 was the approximate location of highest heat flux, and cooling station 22 was the last station in the chamber. The figure shows a similar pattern at both stations and for both chamber pressures. At both stations the heat flux is significantly lower at the lower mixture ratios, but relatively even between mixture ratio of 0.50 and 0.70. It is clear from the figures, however, that the heat flux at station 8 was much higher than at station 22. For a chamber pressure of 2111 kPa, the maximum heat flux at station 8 was 5000 kW/m^2 compared to only 2650 kW/m^2 at station 22. Similarly, for a chamber pressure of 1063 kPa, the maximum heat flux at station 8 was 3200 kW/m^2 compared to only 1450 kW/m^2 at station 22.

To evaluate the axial variation in heat flux, figure 6 shows the experimental heat flux as a function of axial distance from the injector face for both chamber pressures. The mixture ratio for these curves was approximately 0.55. This mixture ratio resulted in the highest heat fluxes, and is also a likely operating point for an actual engine. The figure shows that the heat flux increases steadily from the beginning of the chamber until about 5 to 6 cm into the chamber, where the heat flux then decreases through the rest of the chamber. The graphs of heat flux as a function of axial location were used to determine the location of the end of the combustion zone for each mixture ratio. This was defined as that point showing maximum heat flux. By using this point, it was assumed that the further growth of the boundary layer has a small effect on the location of maximum heat flux.

Figure 7 shows the location of the end of the combustion zone in the chamber for the mixture ratios tested. At lower oxygen to fuel mixture ratios, the combustion zone is shorter, and then becomes longer at the higher mixture ratios. The figure indicates that the combustion zone ended between 2.7 and 6.5 cm (cooling stations 4 and 10). The duration of the combustion could be affected by several parameters, including kinetic reactions and injection velocity ratio. The reaction rate for the CO and O_2 reaction is known to be slow. It is possible that the slow kinetics of the system require more time for enough collisions to occur with sufficient energy to form complete combustion. Specific injector parameters may also affect combustion. With a concentric tube injector, optimum mixing occurs at high fuel-to-oxygen injection velocity ratios. At the lower mixture ratios, more fuel is injected through the outer annulus, and it is therefore injected at a higher velocity. Similarly, at the low mixture ratios, less oxygen is injected through the center orifice, and it is therefore injected at a lower velocity. This combination produces a higher fuel-to-oxygen injection velocity ratio at the lower mixture ratios, promoting mixing, and allowing combustion to be completed more quickly.

Theoretical Analysis. In figure 8 the experimental heat flux as a function of axial distance for a mixture ratio of 0.55 and a chamber pressure of 1070 kPa is shown again. Also included in the figure is the heat flux calculated from two different computer codes.

It can be seen that the experimental heat flux is significantly higher than that calculated by both codes. LPP predicts a high heat flux at the injector face which then decreases throughout the chamber as the boundary layer grows. The REHTEP code uses a Nusselt number correlation for fully developed turbulent flow (equations (1) and (2)) to calculate heat flux. Both codes assume that all energy release in the combustion chamber occurs at the injector.

To further compare the experimental heat transfer results with fully developed turbulent flow, the experimental heat transfer correlation coefficient is shown in figure 9. The dashed line in the figure represents the empirically derived correlation coefficient of 0.026 for cooling in a duct with fully developed turbulent flow. The figure shows that the experimental correlation coefficient is always higher than the 0.026 value. The largest difference occurs at the same location where the highest heat flux was observed (where the combustion zone ends), with an experimental value five times higher than 0.026. These high correlation coefficients would seem to indicate that the combustion process has caused the experimental heat transfer characteristics to behave in a manner different from fully developed turbulent flow. By the end of the chamber, however, the experimental correlation coefficient is only slightly higher than the 0.026 value, and it is possible that at this point the flow in the chamber is more like fully developed turbulent flow.

CONCLUSIONS

The combustion and heat transfer characteristics of carbon monoxide and oxygen combustion were evaluated in a calorimeter combustion chamber with a heat sink nozzle and an eighteen element concentric tube injector. The experimental C* efficiency was between 95 and 96.5 percent over a mixture ratio range of 0.3 to 1.0. This was a significant improvement over a triplet injector design evaluated in a previous test program. Maximum heat flux was approximately 3200 kW/m^2 at a chamber pressure of 1063 kPa and 4900 kW/m^2 at a chamber pressure of 2111 kPa. Using the location of maximum heat flux as an indicator, the end of the combustion zone occurred between 2.7 and 6.5 cm downstream of the injector.

The experimental heat flux and correlation coefficients were much higher than those calculated using a Nusselt type correlation for cooling in a duct with fully developed turbulent flow. More experimentation is needed to further evaluate the results obtained in the calorimeter chamber tests. Experiments with various injector designs and varying chamber lengths are needed to determine the effects of the injection velocity ratio and the slow kinetic reactions of the carbon monoxide and oxygen combination.

REFERENCES

1. Teeter, R.R.; and Crabb, T.M.: Lunar Surface Base Propulsion System Study. NASA CR–171982–VOL–1, 1987.

2 Wickman, J.H.; Oberth, A.E.; Mockenhaupt, J.D.: Lunar Base Spacecraft Propulsion with Lunar Propellants. AIAA Paper 86–1763, 1986.

3. Repic, E., et al.: If We're going to Mars, Why Stop at the Moon? Presented at the Conference, "The Case for Mars IV, The International Exploration of Mars," Boulder, CO, June 1990.

4. Stancati, M.L., et al: In Situ Propellant Production for Improved Sample Return Mission Performance. AAS Paper 79–177, Astrodynamics 1979; Proceedings of the Conference, P. Penzo, et al., eds., Pt. 2, Univelt, Inc., San Diego, CA, 1980, pp. 909–921.

5. French, J.R.: Rocket Propellants from Martian Resources. J. Br. Interplan. Soc., vol. 42, Apr. 1989, pp. 167–170.

6. Zubrin, R.M.; Baker, D.A.; and Gwynne, O.: Mars Direct: A Coherent

Architecture for the Space Exploration Initiative. AIAA Paper 91–2333, 1991.

7. Giudici, B.: A Get Started Approach for Resource Processing. AAS Paper 87–262, The Case for Mars III: Strategies for Exploration—Technical, C.R. Stoker, ed., Univelt, Inc., San Diego, CA 1989, pp. 469–478.

8. Linne, D.L.; Roncace, J.; and Groth, M.F.: Mars In Situ Propellants: Carbon Monoxide and Oxygen Ignition Experiments. NASA TM–103202, 1990 (Also, AIAA Paper 90–1894, 1990).

9. Linne, D.L.: Carbon Monoxide and Oxygen Combustion Experiments: A Demonstration of Mars In Situ Propellants. NASA TM–104473, 1991 (Also, AIAA Paper 91–2443, 1991).

10. Nickerson, G.R.; Dang, A.L.; and Coates, D.E.: Engineering and Programming Manual: Two-Dimensional Kinetic Reference Computer Program (TDX). NASA CR–178628, 1985.

11. Eckert, E.R.G.; and Drake, R.M., Jr.: Heat and Mass Transfer. Second ed., McGraw-Hill Book Co., Inc., 1959.

Table 1. - Location of Coolant Stations and Rib Thermocouples

Coolant Station Number	Axial Location (Distance from Injector Face) (cm)	Thermocouples Inserted in Copper Liner
1	0.546	No
2	1.458	Yes
3	2.093	No
4	2.728	No
5	3.363	Yes
6	3.998	No
7	4.633	No
8	5.268	Yes
9	5.903	No
10	6.538	Yes
11	7.173	No
12	7.811	Yes
13	8.443	No
14	9.078	Yes
15	9.713	Yes
16	10.35	Yes
17	10.98	Yes
18	11.62	Yes
19	12.25	No
20	12.89	No
21	13.52	Yes
22	14.16	No

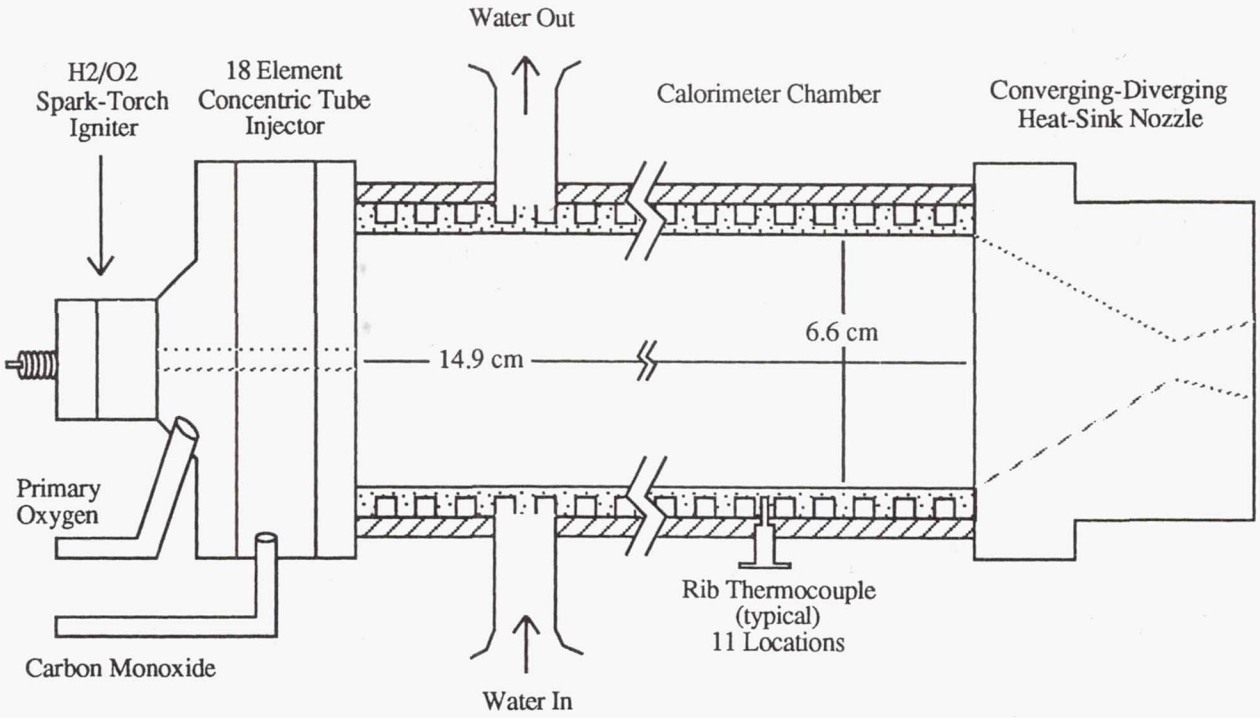

(a) Calorimeter engine assembly.

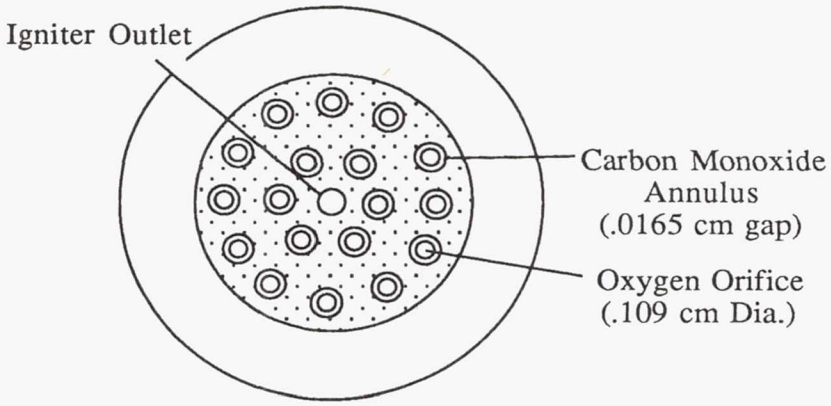

(b) 18 element concentric tube injector face.

Figure 1.—CO/O_2 calorimeter experimental test hardware schematic.

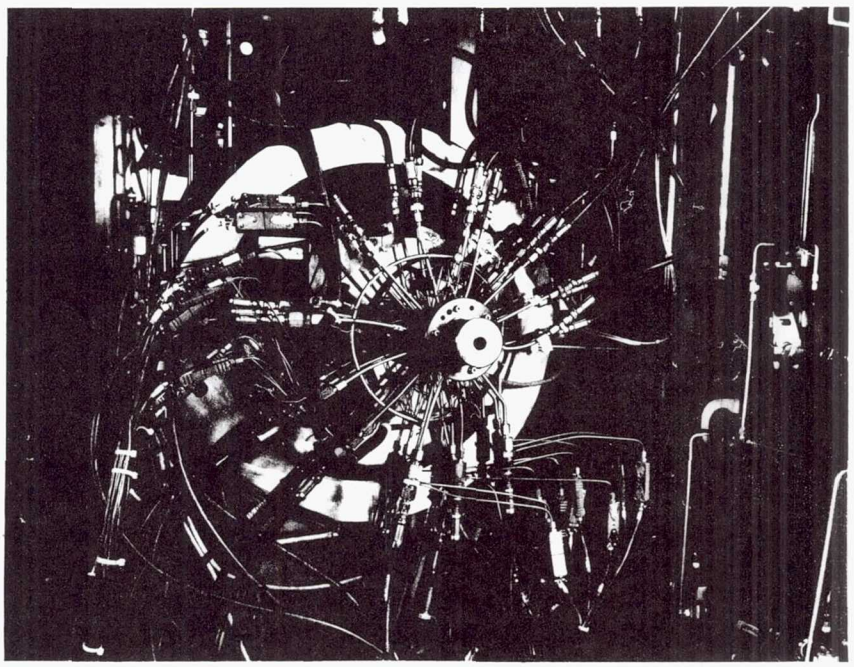

Figure 2.—Calorimeter chamber on test stand.

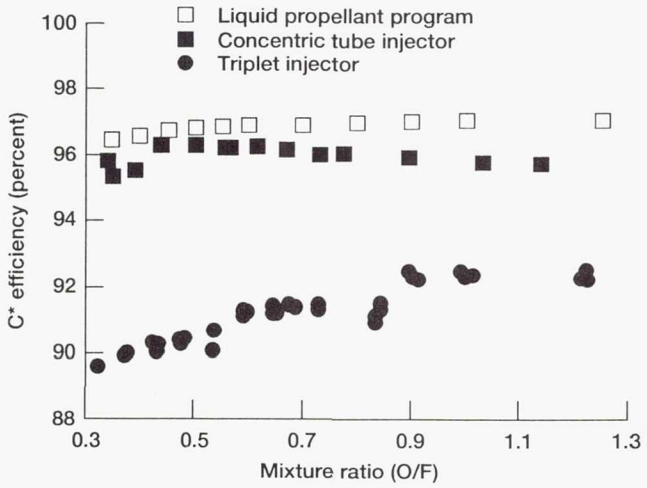

Figure 3.—Comparison of combustion chamber C* efficiencies for triplet and concentric tube injectors.

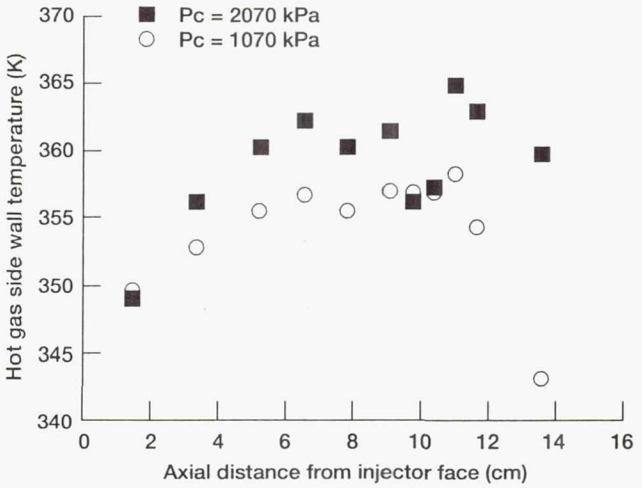

Figure 4.—Comparison of hot-gas side wall temperatures as measured by thermocouples at a depth of 0.076 cm.

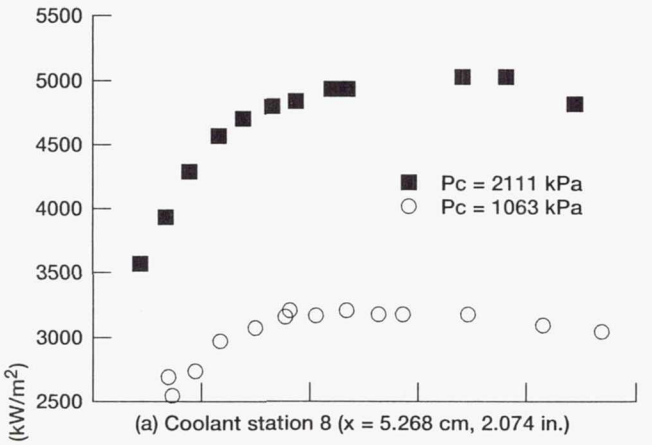

(a) Coolant station 8 (x = 5.268 cm, 2.074 in.)

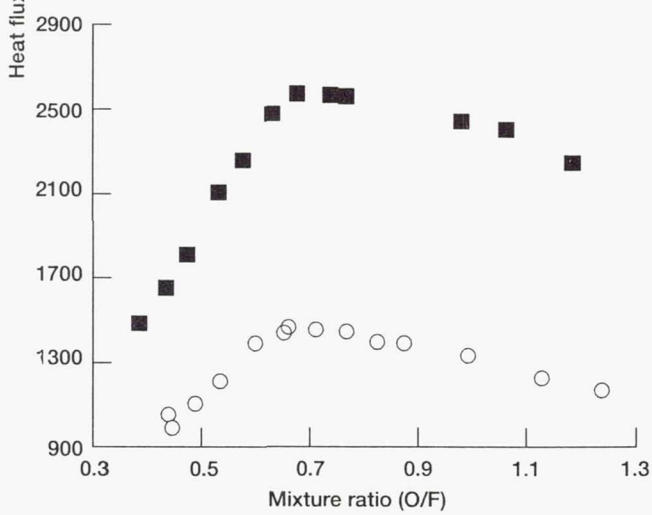

(b) Coolant station 22 (x = 14.16 cm, 5.574 in.)

Figure 5.—Experimental heat flux as a function of mixture ratio for both chamber pressures.

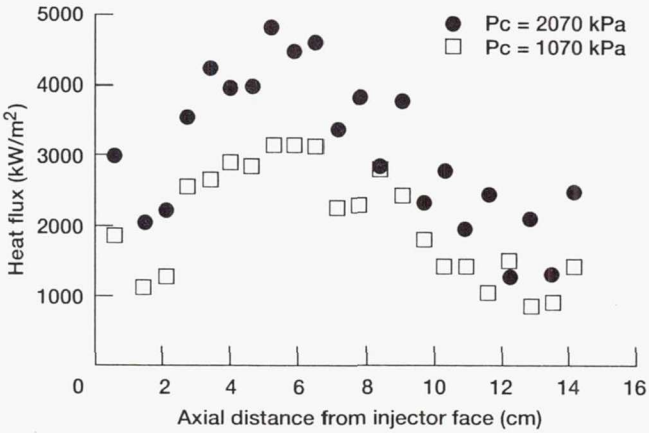

Figure 6.—Experimental heat flux for both chamber pressures (mixture ratio = 0.55).

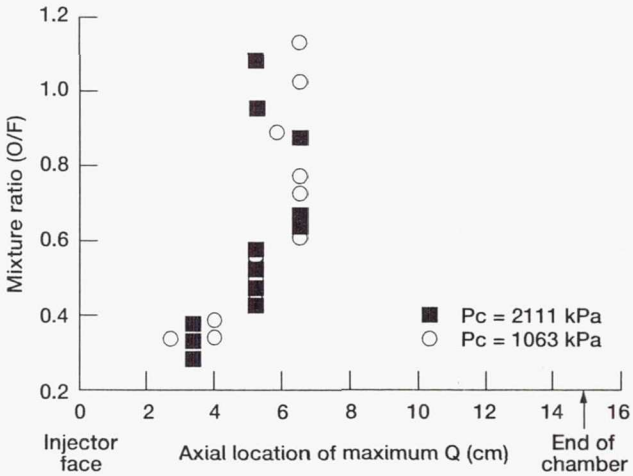

Figure 7.—Location of maximum heat flux for varying mixture ratio.

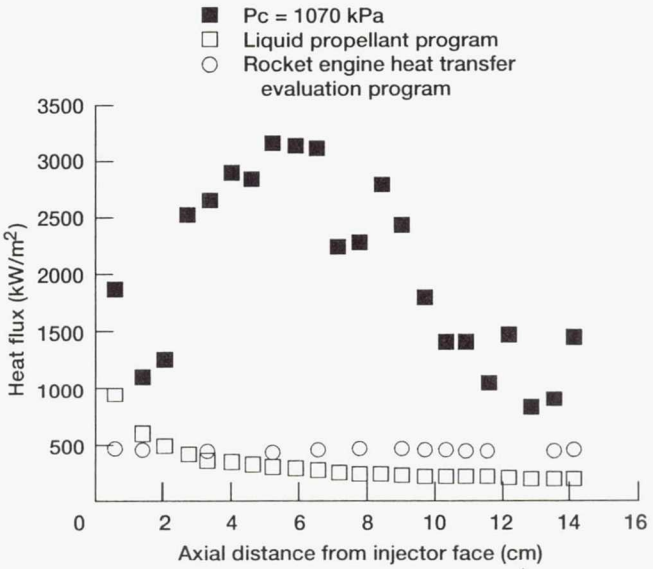

Figure 8.—Comparison of experimental and theoretical heat flux in the chamber (Pc = 1070 kPa, mixture ratio = 0.558).

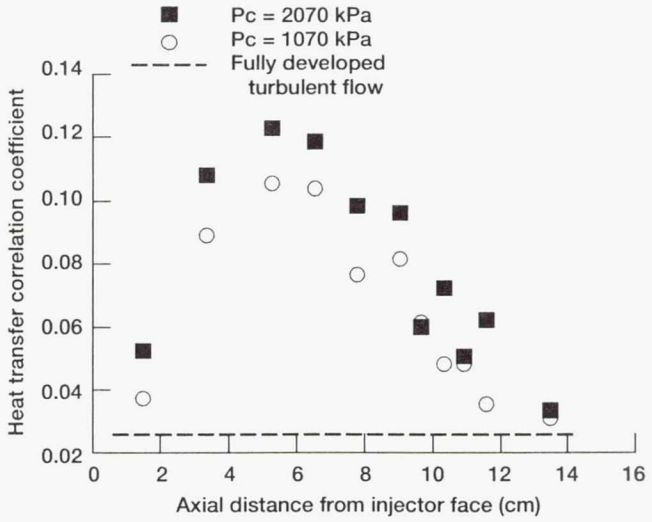

Figure 9.—Experimental heat transfer correlation coefficient in the combustion chamber.

REPORT DOCUMENTATION PAGE

Form Approved
OMB No. 0704-0188

1. AGENCY USE ONLY (*Leave blank*)	2. REPORT DATE	3. REPORT TYPE AND DATES COVERED
	February 1993	Technical Memorandum

4. TITLE AND SUBTITLE

Performance and Heat Transfer Characteristics of a Carbon Monoxide/Oxygen Rocket Engine

5. FUNDING NUMBERS

WU–506–42–72

6. AUTHOR(S)

Diane L. Linne

7. PERFORMING ORGANIZATION NAME(S) AND ADDRESS(ES)

National Aeronautics and Space Administration
Lewis Research Center
Cleveland, Ohio 44135–3191

8. PERFORMING ORGANIZATION REPORT NUMBER

E–7521

9. SPONSORING/MONITORING AGENCY NAMES(S) AND ADDRESS(ES)

National Aeronautics and Space Administration
Washington, D.C. 20546–0001

10. SPONSORING/MONITORING AGENCY REPORT NUMBER

NASA TM–105897

11. SUPPLEMENTARY NOTES

Responsible person, Diane L. Linne, (216) 977–7512.

12a. DISTRIBUTION/AVAILABILITY STATEMENT

Unclassified - Unlimited
Subject Category 20 and 28

12b. DISTRIBUTION CODE

13. ABSTRACT ***(Maximum 200 words)***

The combustion and heat transfer characteristics of a carbon monoxide and oxygen rocket engine were evaluated. The test hardware consisted of a calorimeter combustion chamber with a heat sink nozzle and an eighteen element concentric tube injector. Experimental results are given at chamber pressures of 1070 and 3070 kPa, and over a mixture ratio range of 0.3 to 1.0. Experimental C* efficiency was between 95 and 96.5 percent. Heat transfer results are discussed both as a function of mixture ratio and axial distance in the chamber. They are also compared to a Nusselt number correlation for fully developed turbulent flow.

14. SUBJECT TERMS

Propellent combustion, Extraterrestrial resources, Carbon monoxide, Heat Transfer

15. NUMBER OF PAGES

12

16. PRICE CODE

A03

17. SECURITY CLASSIFICATION OF REPORT	18. SECURITY CLASSIFICATION OF THIS PAGE	19. SECURITY CLASSIFICATION OF ABSTRACT	20. LIMITATION OF ABSTRACT
Unclassified	Unclassified	Unclassified	

National Aeronautics and
Space Administration

Lewis Research Center
Cleveland, Ohio 44135

FOURTH CLASS MAIL

ADDRESS CORRECTION REQUESTED

Postage and Fees Paid
National Aeronautics and
Space Administration
NASA 451

Official Business
Penalty for Private Use $300

NASA